

Heat transfer enhancement in a horizontal channel by the addition of curved deflectors

L. Luviano-Ortiz^a, A. Hernandez-Guerrero^{a,*}, C. Rubio-Arana^a, R. Romero-Mendez^b

^a *Department of Mechanical Engineering, Universidad de Guanajuato, Tampico 912/Apartado Postal 215A, Col. Bellavista, C.P. 36730, Salamanca, Guanajuato, Mexico*

^b *Facultad de Ingeniería, Universidad Autónoma de San Luis Potosí, Av. Dr. Manuel Nava 8, Zona Universitaria, San Luis Potosí, SLP 78290, Mexico*

Received 21 May 2007; received in revised form 19 December 2007

Available online 28 March 2008

Abstract

This paper presents the heat transfer and fluid dynamics analysis of a horizontal channel formed by parallel plates with periodic insertions of heated blocks, having curved deflectors to direct the flow. The heat transfer coefficient investigated is compared with that of the horizontal channel without deflectors. The aim of the deflectors is to lead the fluid to the space between the heated blocks increasing the dynamics in this area. This zone will normally, without deflectors, become a stagnant fluid zone in which low energy transfer rate occurs. The results show that the heat transfer coefficient is larger as compared to that of the case without deflectors. The increment in the heat transfer coefficient is due primarily to the fluid motion stirred in the area between the heated block due to the deflectors. However, it must be pointed out, this implementation also increases the pressure drop in the channel.

© 2008 Elsevier Ltd. All rights reserved.

1. Introduction

Theoretical and experimental investigations have been carried out to understand the heat transfer and the geometry relation in horizontal channels formed by parallel flat plates since an improvement implies energy savings, and by consequence a lessening in process equipment, greater efficiency and greater control over the process. Attempts have been made to increase the heat transfer by trying different configurations, roughness on the plate surfaces, adding fins or even annexing deflectors which affect the direction of the flow [1–5]. The main objective is to cause instability in the flow in order to reduce the thickness of the thermal boundary layer and to increase the convective coefficients.

The grooved channel system is characteristic of a wide class of engineering heat exchange problems (heat transfer surfaces of heat exchangers, nuclear reactors cores, mass transfer equipment, etc.), and in this study it represents a

simplified two-dimensional model of coolant flow over an electronic circuit board with heated chips. In most electronic cooling applications the design requires that the temperatures of the heated components remain below a prescribed level for a given imposed heat flux. In order to satisfy this maximum temperature requirement, two approaches can be pursued. In the first approach, which is suitable for applications where heat removal requirements are moderate, the flow rate of the coolant can be increased while accepting a given flow topology. This solution is limited, for example, by noise generated by the cooling system and by the pumping power that can be delivered with the selected hardware responsible for transporting the coolant [1]. An alternative approach involves the modification of the channel topology while keeping fixed the flow rate of the coolant. This becomes the solution of choice when minimizing the pumping losses and other drawbacks associated with high volume flow rates, such as fan noise. When either of the two approaches can achieve the required heat transfer coefficient, the selection can be made based on optimization criteria accounting for the overall system performance (which includes manufacturing and

* Corresponding author. Tel.: +52 464 64 80911; fax: +52 464 64 72400.
E-mail address: abelh@salamanca.ugto.mx (A. Hernandez-Guerrero).

Nomenclature

D_h	hydraulic diameter, $2s$	s	space between the plates at the entrance of the channel
f	friction factor	T_b	temperature of the fluid at the entrance
h	convective heat transfer coefficient, $W/(m^2 K)$	T_w	upper and lower temperature of the plates
K	thermal conductivity	U	dimensionless velocity in the X -axis
MN	maximum value	u	average velocity in the X -axis
MX	minimum value	V	dimensionless velocity in the Y -axis
Nu	local Nusselt number	v	average velocity in the Y -axis
\bar{Nu}	global Nusselt number	v_{in}	entrance velocity
P	dimensionless pressure		
Pr	Prandtl number		
q''	heat transfer rate	<i>Greek symbols</i>	
Q	dimensionless heat transfer	α	thermal diffusivity
R	radius of the deflector	ν	fluid kinematic viscosity
R_x	position of the deflector in the X -coordinate	μ	fluid dynamic viscosity
R_y	position of the deflector in the Y -coordinate	θ	dimensionless temperature
Re_D	Reynolds number based on the hydraulic diameter, $V_{in}D_h/\nu$		

economic considerations). This paper presents numerical results reflecting an approach that accounts for both the heat transfer and the pressure drop effects.

Previous studies have demonstrated that the heat transfer along a horizontal channel consisting of parallel flat plates with periodic insertion of heated blocks is low due to the stagnation of the flow in the region located between consecutive blocks, since the square geometry does not allow the flow right after the block to move, forcing it to be stagnant [1–4]. The increase in the heat transfer in this type of channel depends largely on the cooling of the lateral walls of the heated blocks where the flow is trapped. Therefore, finding the means to improve the heat transfer in the horizontal channel of parallel flat plates will result in an improved performance. In a horizontal channel formed by parallel flat plates, the fluid and the thermal boundary layer develop along the length of the surface of heated blocks, which periodically stands out in the main flow of the channel. Once the flow passes over the upper surface of the blocks it is directed to the region located between consecutive blocks, but mainly hitting the next block. However, at the same time that the fluid is heated, it gets trapped in this area and creates a slow and recirculating flow. The method to increase the heat transfer considered in this study falls into the area of practical applications due to its simplicity, reliability and relatively low cost.

2. Background

Tuckerman and Pease [16] from Stanford University first introduced the concept of a heat dissipater for extremely large heat rates in an article published in 1981. Since then, other researchers have published experimental or theoretical works and have generated a significant quantity of information in the area of heat transfer dissipation.

Amon and Mikic [6] and Farhanieh et al. [7] have addressed the problem of heat transfer in grooved channels, and the results of these studies indicate that the redevelopment of the thermal boundary layer along the top surface of each heated block, inherent in electronic cooling applications, is accompanied by high heat transfer coefficients. The slow recirculating flow in the groove is heated by both upstream and downstream blocks, and its interaction with the colder main channel flow is impeded by the shear layer spanning the groove. Thus diffusion is the dominant heat transfer mechanism between the groove region and the main channel flow [7,8]. It was found that in some situations, depending on the channel geometry, flow velocity and thermal boundary conditions, heat transfer in developing flow in a grooved channel can even be lower than that in the limiting case of fully-developed flow in a similar asymmetrically heated parallel plate channel [7]. For example, the spacing between the blocks and the block dimensions relative to the channel dimensions influence both the magnitude of heat transfer and associated pressure drop. Clearly, the need to develop strategies that would improve heat transfer in grooved channels provides the motivation to explore new solutions suitable for the improvement of thermal control of electronic equipments.

Past research has revealed that heat transfer in grooved channels can be enhanced through improving lateral mixing by disrupting the shear layer separating the bulk flow and the recirculating flow, and thus destabilizing the transversal vortex in the groove [1–4]. Herman and Kang [1,3] reported results of a comparative evaluation of three heat transfer enhancement strategies for forced convection cooling of a parallel plate channel populated with heated blocks, representing electronic components mounted on printed circuit boards. Heat transfer in the reference geometry, the asymmetrically heated parallel plate channel, was

compared with that of the basic grooved channel, and the same geometry enhanced by cylinders and vanes placed above the downstream edge of each heated block. Heat transfer in the grooved channels enhanced with cylinders and vanes showed an increase by a factor of 1.2–1.8 and 1.5–3.5, respectively, when compared to data obtained for the basic grooved channel; however, the accompanying pressure drop penalties also increased significantly.

Ko and Anand [9] developed an experimental investigation to measure module average heat transfer coefficients in uniformly heated rectangular channel with wall-mounted porous baffles. Baffles were mounted alternatively on the top and bottom of the walls. Heat transfer coefficients and pressure loss for periodically fully-developed flow and heat transfer were obtained for different types of porous medium. The use of porous baffles resulted in heat transfer enhancement as high as 300% compared to heat transfer in straight channel with no baffles. Experiments showed that the flow and heat transfer reached periodically fully-developed state downstream of the seventh module. Liu and Chen [10] experimentally studied turbulent heat transfer and fluid flow in a rectangular channel with perforated ribs. Consideration was given to both attached (to wall) and detached ribs. Perforated ribs were made up of aluminum. Their study indicated that the highest Nusselt number was around three (3) times larger than that for a corresponding channel without ribs.

Molki and Mostoufizadeh [11] developed an experimental study to investigate heat transfer and pressure drop in a rectangular duct with repeated-baffle blockages. The baffles were arranged in a staggered fashion with fixed axial spacing. The test duct had a rectangular cross-section and the baffle blockages were installed on the upper and lower walls of the duct in a staggered manner. In this orientation, each baffle from one wall was situated in the cross-sectional plane which passed through the midpoint of the baffles on the opposite wall. The staggered arrangement thus obtained provided a zigzag path for the core and created the recirculating zones near the walls of the duct and between the neighboring baffles. The transfer coefficients were evaluated in the periodic fully-developed and entrance regions of the duct. The presence of the baffles enhanced these coefficients. The pressure drops were also investigated, and it was found that the baffles increase the pressure drop much faster than they increase the mass and heat transfer coefficients.

Billen and Yapici [5] carried out an experimental investigation to study the enhancement of the heat transfer from a heated flat plate with rectangular blocks at different orientation angles. Their results indicated that the heat transfer could be enhanced depending on the spacing between blocks, and the block orientation angle. The maximum heat transfer rate was obtained at the orientation angle of 45°. Further experimental investigations and numerical modeling by Amon and Mikic [6], Amon et al. [12], Farhanieh et al. [7] and Herman and Kang [1,2], indicated that the redevelopment of the thermal boundary layer along

each heated block, inherent in electronic cooling applications, was accompanied by high heat transfer coefficients. However, the overall heat transfer along one heated block-groove periodicity unit was low due to the inefficient groove region. Warm fluid was trapped in the slow recirculation flow in the groove, heated by both upstream and downstream blocks, with diffusion being the dominant heat transfer mechanism over the shear layer between groove region and main channel flow [1,2,7,8]. They implied that one of the possibilities to enhance heat transfer in grooved channels was to improve lateral mixing by disrupting the shear separating the bulk flow and the recirculating flow in the groove and introducing vertical components in this region.

Adachi and Uehara [13] conducted the linear stability analysis of flow in a channel with periodically grooved parts by using the spectral element method. The channel was composed of parallel plates with rectangular grooves on one side in a streamwise direction. The flow field was assumed to be two-dimensional and fully-developed. At a relatively small Reynolds number, the flow was in a steady-state, whereas a self-sustained oscillatory flow occurred at a critical Reynolds number as a result of Hopf bifurcation due to an oscillatory instability mode. The critical Reynolds number could be determined by the sign of a linear growth rate of the eigenvalues. It was found that the bifurcation occurs due to the oscillatory instability mode which has a period two times as long as the channel period.

Herman and Kang [1–3] identified six characteristic regions of interest in the study of incremental heat transfer in horizontal channels of parallel flat plates with inserted blocks. These regions are illustrated in Fig. 1a. Herman and Kang [2,3] were able to increase the heat transfer in the horizontal channel of parallel flat plates with the periodic insertion of blocks heated through the addition of cylinders in which the fluid was accelerated towards region IV. This acceleration was caused by the addition of the cylinders downstream along the edge of the heated block. The heat transfer in this channel increased by a factor of 1.2–1.8 when compared to the horizontal channel formed by parallel flat plates. However, no increase of heat transfer

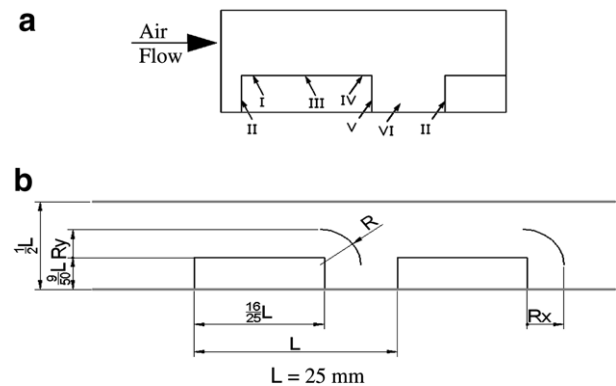


Fig. 1. Sketch of the geometry under analysis (a) regions of interest [3] and (b) significant parameters.

was obtained in region V, and the increase of heat transfer was only moderate in region II. The cooling of these regions is the subject of the present study.

The main reason for the introduction of curved deflectors along the downstream edge of the heated block is to increase the heat transfer in regions II, IV and V, since the deflector accelerates the flow and directs it to the region between the blocks as illustrated in Figs. 1b and 2. Deflectors are commonly used to control the flow in pumps and turbines [1–4]. In tubes, conduits and similar applications to the present study, the deflectors reduce the flow separation. In horizontal channels of parallel flat plates with periodic insertion of heated blocks, the deflectors allow a greater heat transfer towards the fluid from the area between the blocks.

Anderson and Moffat [14] used curved vanes (which they called “scoops”) to improve the cooling of discrete electronic components through increased thermal mixing in the coolant flow. In order to reduce air temperatures near electronic components, they installed small “scoops” on the bottom of the groove, in the regions of high temperature and low velocity. The “scoops” were oriented such to direct the flow out of the groove (as opposed to deflecting it into the groove, as in the present study) with the aim to enhance mixing and reduce temperature non uniformity. Anderson and Moffat [14] found that their approach induces smaller pressure drop than conventional turbulators for a given decrease of the operating temperature.

Fu and Tong [15] performed a numerical study on the influence of heat transfer of an oscillating cylinder located at the entrance to the horizontal channel with periodical heated blocks. In addition they analyzed the effects of the Reynolds number, the amplitude and the frequency of oscillation of the cylinder on the heat transfer. The results demonstrated that the heat transfer from the heated blocks increased surprisingly when the frequency of oscillation of the cylinder was found in the region near the top of the block. Furthermore it was demonstrated that when the cylinder is oscillating, the heat transfer increases 120% compared to the case when there is no cylinder in the horizontal channel.

Adachi and Hasegawa [17] numerically studied the transition of the flow in a periodically grooved channel for periodicity indices $m = 1$ up to 6 by assuming the two-dimensional and fully-developed flow field, where m was defined as a number of grooves in which the flow

repeats periodically. Critical Reynolds numbers for the onset of a self-sustained oscillatory flow from a steady-state flow were evaluated by numerical simulations.

In this study three different sizes of deflectors were analyzed and placed at different positions in the grooved channel, to be able to determine the deflector size – and its location – that generates the best heat transfer. An analysis of the pressure drops generated by all configurations was performed as well, trying to determine the best trade-off of largest heat transfer and smallest pressure drop.

3. Geometry of the channel and physical situation

The channel used in this study contained ten blocks in its inside. A section of the geometry of this channel as well as its physical dimensions is presented schematically in Figs. 1b and 2. The key physical dimensions are indicated in Fig. 1b. The addition of deflectors causes acceleration of the flow trapped between the blocks.

In this study the dimensions represented by R_x and R_y were optimized to obtain the highest heat transfer. This study aims to explore the effect of the deflector located over the final part of the heated block. Hence, three different sizes of deflectors are studied ($R = 3L/25, 4L/25, L/25$) in multiple positions (R_x, R_y). Since the current tendency in the use of this type of channel consists of increasingly smaller spaces, no section is considered sufficiently large to guarantee that the flow will reach the beginning of the section of heated blocks completely developed. The work fluid used is air and was considered Newtonian with constant properties, with the flow in the laminar regime and not compressible, without considering the viscosity dissipation in the energy equation and the effects of gravity. The Prandtl number (Pr) characteristic for the fluid is 0.708. The properties of the fluid are considered constant due to previous studies, in which it was shown that the changes in these are insignificant [1]. The working fluid is subjected to a constant flow of heat which is applied on the blocks in the channel.

4. Mathematical analysis

The governing equations for this steady-state conditions and 2D laminar flow model can be treated in a dimensional form by means of the following parameters:

$$\begin{aligned} X &= \frac{x}{s}, & Y &= \frac{y}{s}, & U &= \frac{u}{V_{in}}, & V &= \frac{v}{V_{in}}, \\ P &= \frac{p - p_{in}}{\rho V_{in}^2}, & \theta &= \frac{T - T_{in}}{T_{in}}. \end{aligned} \quad (1)$$

The governing equations written in dimensional form are therefore:

Continuity equation:

$$\frac{\partial u}{\partial x} + \frac{\partial v}{\partial y} = 0. \quad (2)$$

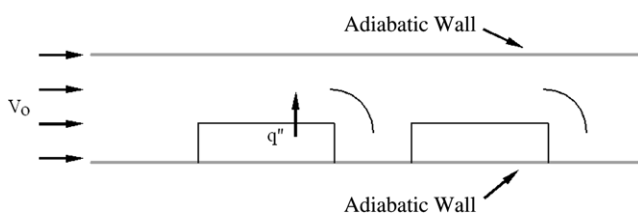


Fig. 2. Configuration of the channel of flat plates with implementation of deflectors.

Momentum equations:

$$\begin{aligned} u \frac{\partial u}{\partial x} + v \frac{\partial v}{\partial y} &= -\frac{\partial p}{\partial x} + \nu \left(\frac{\partial^2 u}{\partial x^2} + \frac{\partial^2 u}{\partial y^2} \right), \\ u \frac{\partial u}{\partial x} + v \frac{\partial v}{\partial y} &= -\frac{\partial P}{\partial y} + \nu \left(\frac{\partial^2 v}{\partial x^2} + \frac{\partial^2 v}{\partial y^2} \right). \end{aligned} \quad (3)$$

Energy equation:

$$\left(u \frac{\partial T}{\partial x} \right) + \left(v \frac{\partial T}{\partial y} \right) = \alpha \left(\frac{\partial^2 T}{\partial x^2} + \frac{\partial^2 T}{\partial y^2} \right) \quad (4)$$

These equations are solved numerically for a Reynolds number (Re_D) range between 490 and 1000 and a Prandtl number of 0.708. The Reynolds number (Re_D) is based on the hydraulic diameter $D_h = 2s$ ($s = 0.010$ m), where s represents the space between plates.

The average Nusselt number was determined as

$$\overline{Nu} = \frac{2\bar{h}s}{k}, \quad (5)$$

where \bar{h} is obtained by means of

$$\bar{h} = \frac{1}{A} \int_A h dA_s. \quad (6)$$

The friction coefficient was determined as

$$f = \frac{\Delta p}{2\rho u_{in}^2}, \quad (7)$$

where Δp is the pressure gradient between the entrance and the exit of the duct.

In order to evaluate the integral given by Eq. (6), the integral trapezoidal numerical method was used. The convective coefficient is defined locally, along the lower channel surface, blocks included.

5. Boundary conditions

The outlet boundary conditions consider the flow exits to the atmosphere. The appropriate boundary conditions for the entrance section are fixed constant uniform velocity, constant fixed ambient temperature, non-slip conditions at the wall, and constant inlet pressure, thus the dimensionless variables for the problem reduce to

$$U = 1; \quad V = 0; \quad \theta = 0; \quad P = 0. \quad (8)$$

The combined channel is affected by a constant influx of heat coming from the blocks, thereby increasing the temperature of the incoming fluid. The boundary conditions considered for these combined plates are

$$U = 0; \quad V = 0; \quad Q = 1. \quad (9)$$

6. Numerical analysis

Numerical simulations were tested by varying the number of computational elements. Likewise, a stability analysis was made in the mesh (testing different configurations) in order to increase stability and reliability of the results [17]. It was determined that the convergence of the finite element model is more stable for a mesh between 9000 and 11,000 elements, also a triangular grid was used since it proved to be the most adequate for the proposed geometry this is shown in Fig. 3.

The computational element for the simulation is an element that is used when it is required to analyze thermal systems and for systems that have fluid and solid regions. The viscous flow and energy equations are solved in the fluid region, while only the energy equation is solved in the solid region. Therefore this element is capable of solving temperature and flow velocity gradients in a region.

A segregated sequential solver algorithm is used, that is, the matrix system derived from the finite element discretization of the governing equation for each degree of freedom is solved separately. The flow problem is nonlinear and the governing equations are coupled together. The sequential solution of all the governing equations, combined with the update of any temperature- or pressure-dependent properties, constitutes a global iteration. The number of global iterations required to achieve a converged solution may vary considerably, depending on the size and stability of the problem. It was estimated that the solution converged once the variation of the variables was of the order of 1×10^{-4} .

7. Results of the hydrodynamic and thermal behavior of the fluid

In Fig. 4a the velocity vectors show the recirculation flow generated between the blocks when there are not deflectors, showing a large flow stagnation in this region.

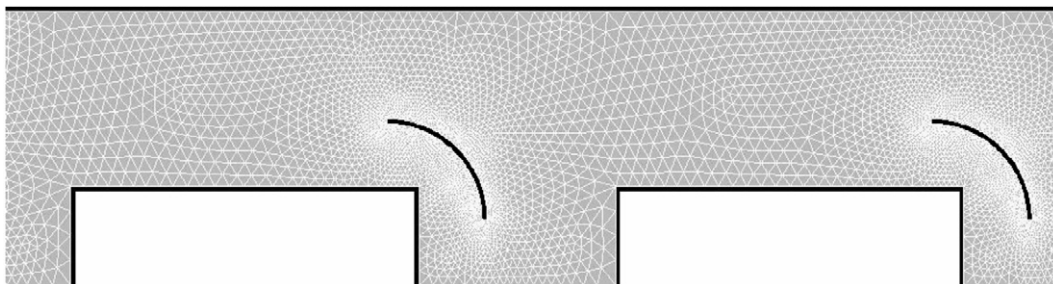


Fig. 3. Scheme of the most optimized mesh used for the analysis.

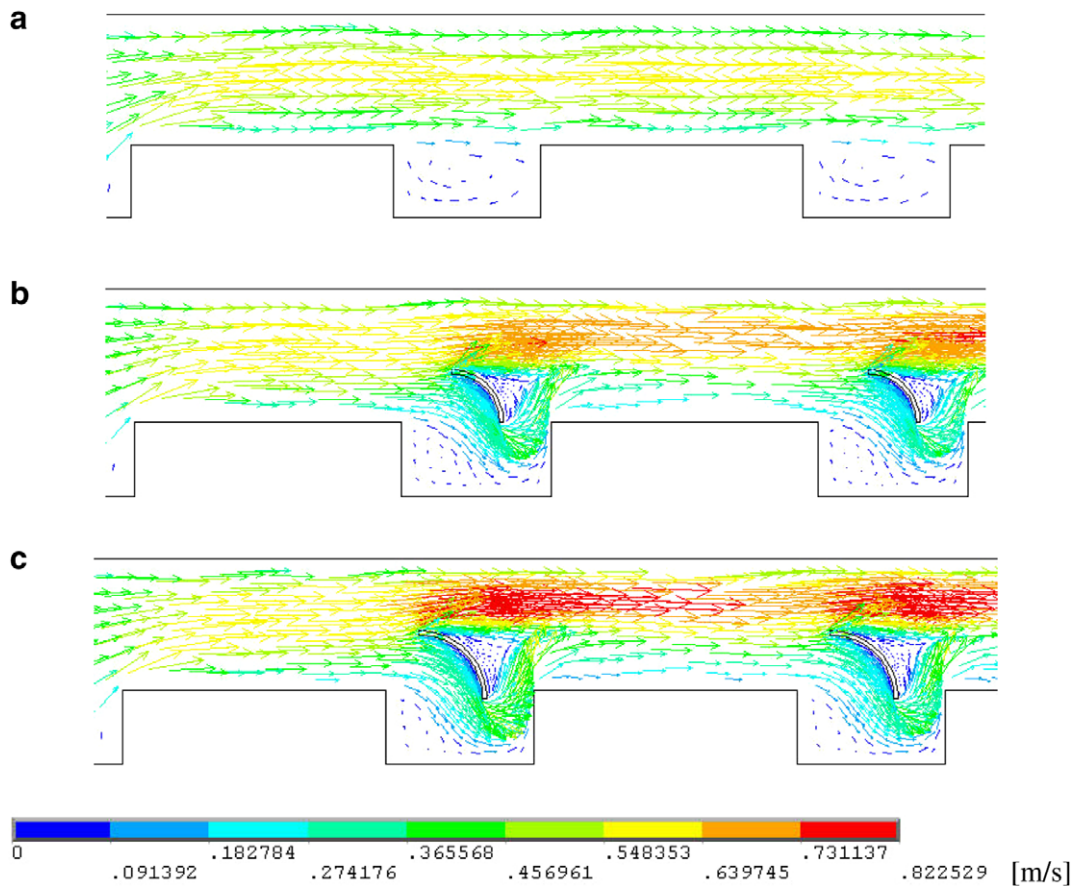


Fig. 4. Velocity vectors between the blocks 6 and 7 for different sizes of deflectors and $Re = 490$: (a) without deflector, (b) $R = 3$ mm, (c) $R = 4$ mm, (d) $R = 5$ mm.

Fig. 4b–d shows the velocity vectors when the deflector propels the flow towards the region between the blocks. Fig. 4b shows that the deflector of 3 mm directs only a small amount of the flow towards the region between the blocks. By comparing Fig. 4b–d, it is possible to observe that the deflectors of greater size will direct a greater amount of flow to the region between the blocks; however, using a greater deflector causes the pressure drop to increase. For all results shown in Fig. 4 the Reynolds number used was 490.

If the deflector is placed at a position near the regions IV and V of Fig. 1a, the flow deflected towards the region between the blocks will immediately go up after passing the deflector causing that the flow would not reach region II (Fig. 1a); this generates a recirculation flow next to region II. Fig. 4b–d shows the deflector at locations closer to region II (far from regions IV and V). These positions will allow that once the flow has passed below the deflector it reaches the region II.

It is noteworthy to observe that, although the deflector is placed at the most suitable locations, the flow recirculation will not be eliminated completely. In a separate section ahead some diagrams are presented showing what the best or worst positions for the deflectors are (for example which positions give small or large recirculation.)

7.1. Velocity contours

It should be kept in mind that the main variables in this proposed configuration are the size and the position of the curve deflector (R_x, R_y) in the channel.

The comparison of the results considered for a laminar Reynolds number (Re_D) of 490 and using velocity contours (Fig. 5). Experimentally, Herman and Kang [1], found that the transition from stable to oscillating fluid occurs near $Re_D = 450$.

Fig. 4 demonstrates the velocity contours for a $R_x = 13L/50$ and $R_y = 3L/25$. It can be observed that the maximum velocity occurs for a channel that has a size deflector of $R = L/5$ and the minimum for $R = 0$. By comparing the maximum velocities for $R = L/5$ and $R = 0$, a 27% difference is found. It is observed that the flow is directed by the deflector to the zones located between the blocks, confirming that the deflector accomplishes the desired objective. It could be observed that the minimal stagnation occurs in the channel with the largest deflector.

7.2. Pressure contours

It is important to know the effects of the parameters involved in this analysis on the pressure contours, because

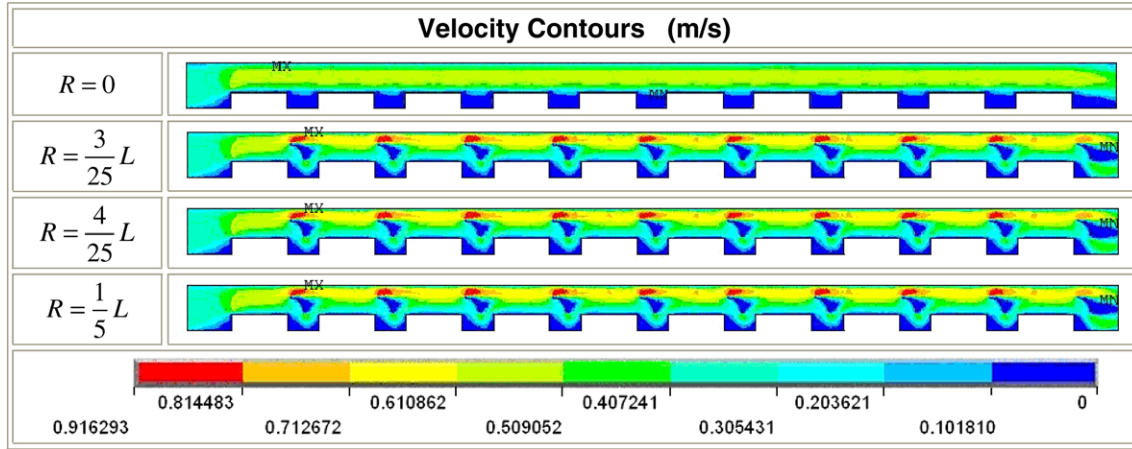


Fig. 5. Velocity contours for $Re_D = 490$ and different sizes of the deflectors.

in addition to other results, this type of channel may be recommended or not based on the trade off of the heat transfer increment vs. a larger pressure drop.

Fig. 6 shows the pressure field for a Reynolds number (Re_D) of 490 and different sizes of the deflector. A point by point comparison found that the maximum values of pressure (MX), as seen in this figure, are at the entrance to the channel, and that the minimum values (MN) are at the exit as would occur in any channel. Therefore, comparing the images of the figure and their correspondent values, it is observed that there is a greater drop in pressure in the channel with the deflector size $R = L/5$ and a smaller drop in pressure for the channel without a deflector.

Upon analyzing the drops in pressure for a deflector of the same size at different positions, a logical pattern was found since increasing the position in R_y , the drop in pressure also increases.

As would be expected, for large size deflectors having the same Reynolds number (Re_D), the drop in pressure is large as well. The same behavior occurs for the deflectors at any position.

It can be concluded that in these types of channels, due to their geometry, the maximum pressures are concentrated over the first heated block for any configuration analyzed. The maximum values for pressure drop at the same Reynolds number (Re_D) occur for the channel with the deflector $R = L/5$ and the smallest pressure drop occurs for the channel with the deflector $R = 3L/25$.

7.3. Temperature contours

For the initial comparison of the temperature contours the same criteria as for the velocity and pressure limits is taken, comparing at the same Reynolds number (Re_D) and for different sizes of deflectors (see Fig. 7). It can be noted that the maximum temperature occurs when $R = 0$, and the minimum temperature when $R = L/5$. Recalling that in Fig. 5 the maximum velocity occurs in the channel with the $R = L/5$ deflector, it can be inferred that there is a greater heat transfer for this channel. This difference in temperature corresponds about 10% in comparison to the

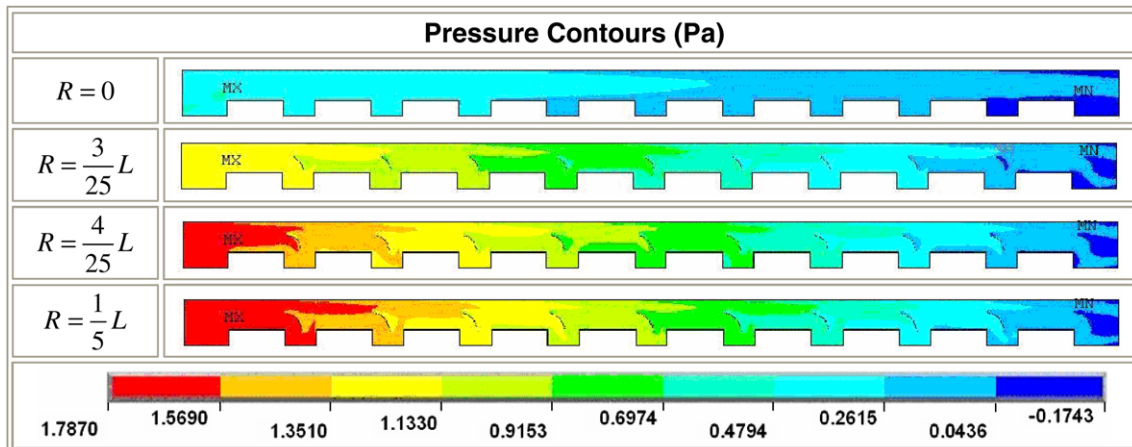


Fig. 6. Pressure contours for $Re_D = 490$ and different sizes of the deflectors.

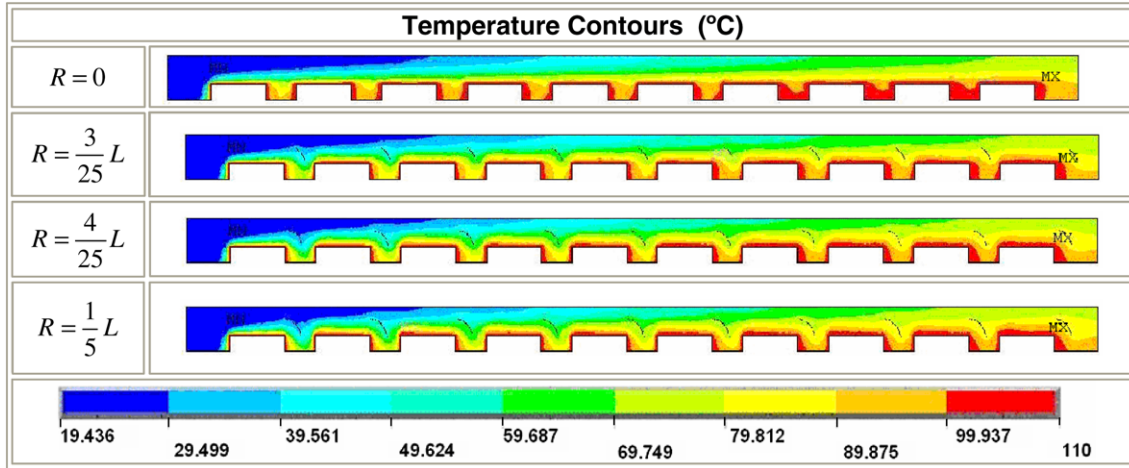


Fig. 7. Temperature contours for $Re_D = 490$ and different sizes of the deflectors.

largest temperature, meaning that the location of the deflector in the channel has a great influence on it.

In Fig. 7 an increase in temperature is observed with a decrease in the size of the reflectors. This is because a smaller deflector directs a lesser quantity of flow to the parts to be cooled. Furthermore, an increase in temperature of the fluid exists in the regions located between the blocks that are due to the recirculation of the flow in these zones, thereby diminishing the heat transfer.

8. Functionality of the deflector

Since the objectives of this study are to determine the position of the deflector (R_x, R_y), and deflector size for

the best possible operation and heat exchange, in order to know the positions where the deflector would be most functional, the diagrams shown in Figs. 8–10 are used. These diagrams enable to determine these positions vs. the deflector size by means of a scale that range from “good” to “bad”, in these diagrams all configurations analyzed in this work are considered.

To determine the functionality of the deflectors the region located between blocks 6 and 7 was chosen, and all cases analyzed. It was considered that the deflector is functional if the average temperature of the region is of the order of $80\text{ }^\circ\text{C}$ (if this criterion was reached the configuration was given a “good” in the diagrams scale); in a likewise manner, it was determined that the configuration

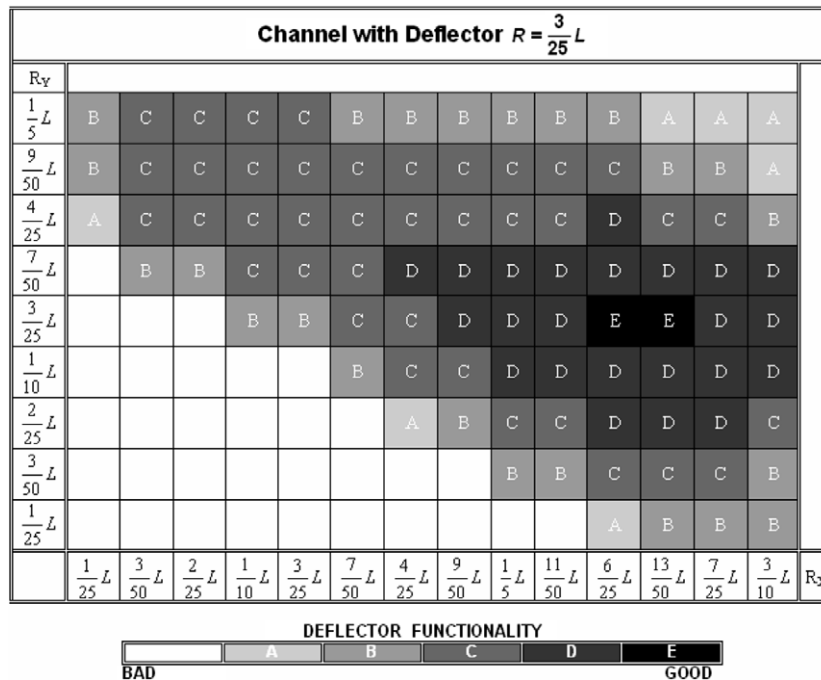


Fig. 8. Functionality of the deflector $R = 3L/25$ for different positions in the channel.

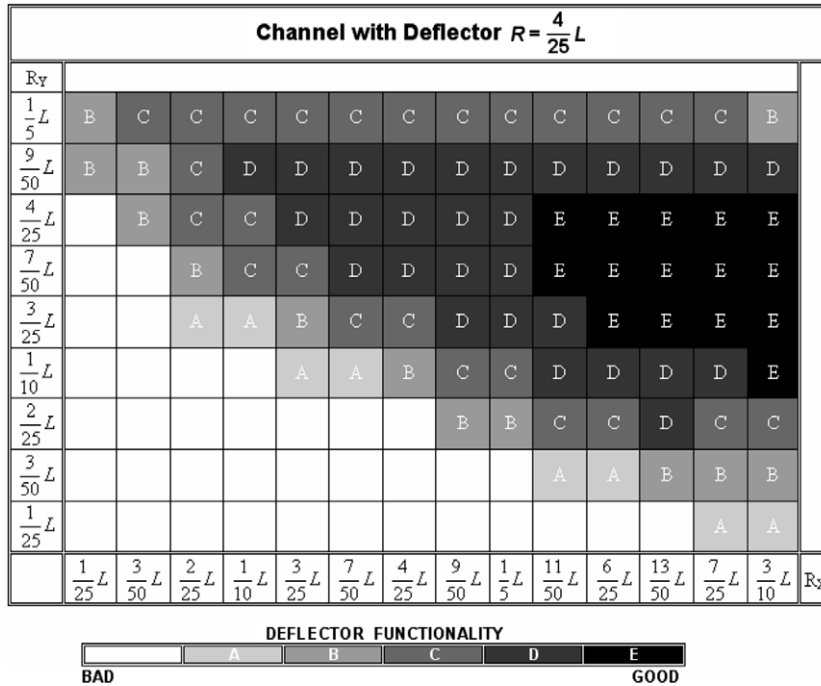


Fig. 9. Functionality of the deflector $R = 4L/25$ for different positions in the channel.

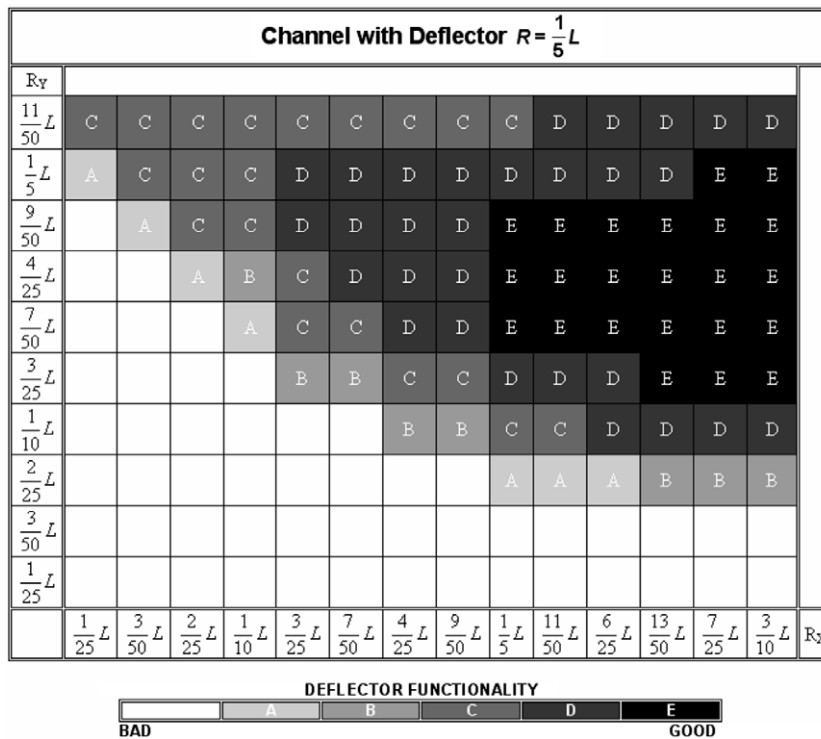


Fig. 10. Functionality of the deflector $R = L/5$ for different positions in the channel.

was not functional if the average temperatures were larger than 100 °C (“bad” in the diagrams scale.) This criterion was used since in the conventional no-deflector channel the temperature in this region reached 105 °C, and the lowest temperature found in this region when using the deflectors was 80 °C. In the diagrams shown in Figs. 8–10, the

scale “good” shows a full dark color and the letter E, whereas the “bad” mark is a full white color with no letter. Full white “bad” mark starts at 100 °C and from there 5 “subscales” are used (A, B, C, D, E), each one representing $(100 - 80)/5$ °C decrease, reaching the final range of “good” and the letter E, which ends at 80 °C.

These diagrams are very useful, since a quick look enables the determination of several possible configurations that will be safe and optimum (around the 80–84 °C range.)

9. Local and global Nusselt number

Fig. 11 shows a comparison of the local Nusselt number for different sizes of the deflectors with the same Reynolds number (Re_D), and in the position $R_x = 6L/25$ and $R_y = 7L/50$ for block 6.

Note: Figs. 11 and 12c, for the sake of illustrating that the results are for the back side of a heated block, the

Y-axis scale and title have been placed on the right-hand side of those figures.

Another parameter that strongly influences the behavior of heat transfer is the Reynolds number (Re_D). In Fig. 12 it is observed that there is a great difference in the local Nusselt number (Nu) for the Reynolds number (Re_D) range analyzed. Fig. 13 shows the variation of the global Nusselt number with respect to the Reynolds number.

Figs. 11 and 12 show that by having deflectors the local Nusselt number increases. Figs. 11 and 12a show that the largest local Nusselt number appears at the beginning of the block heated in its horizontal surface, this is due to the acceleration of the fluid caused by the deflector. As it

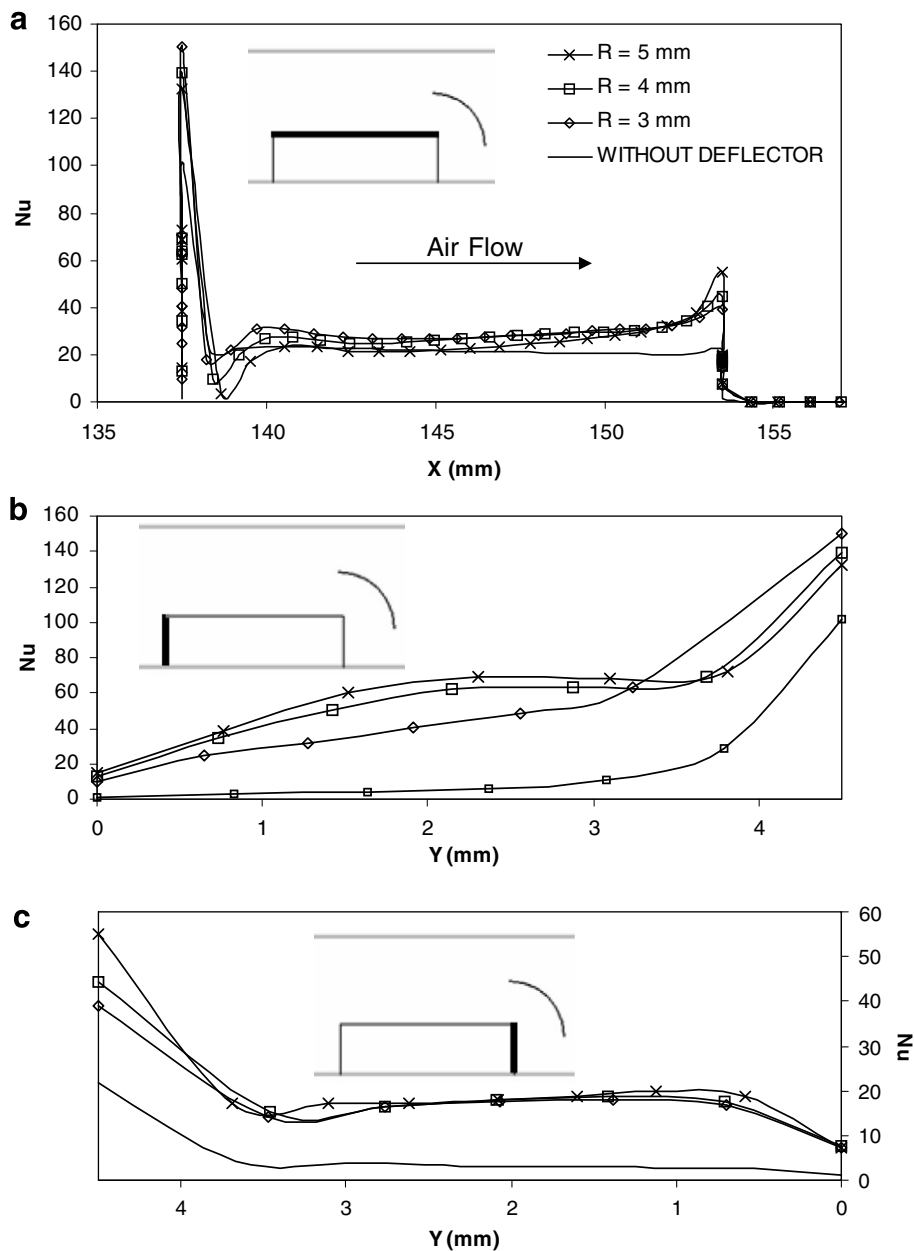


Fig. 11. Local Nusselt number for block 6 with $Re_D = 490$ and different sizes of deflectors: (a) horizontal wall, (b) vertical front wall, (c) vertical back wall.

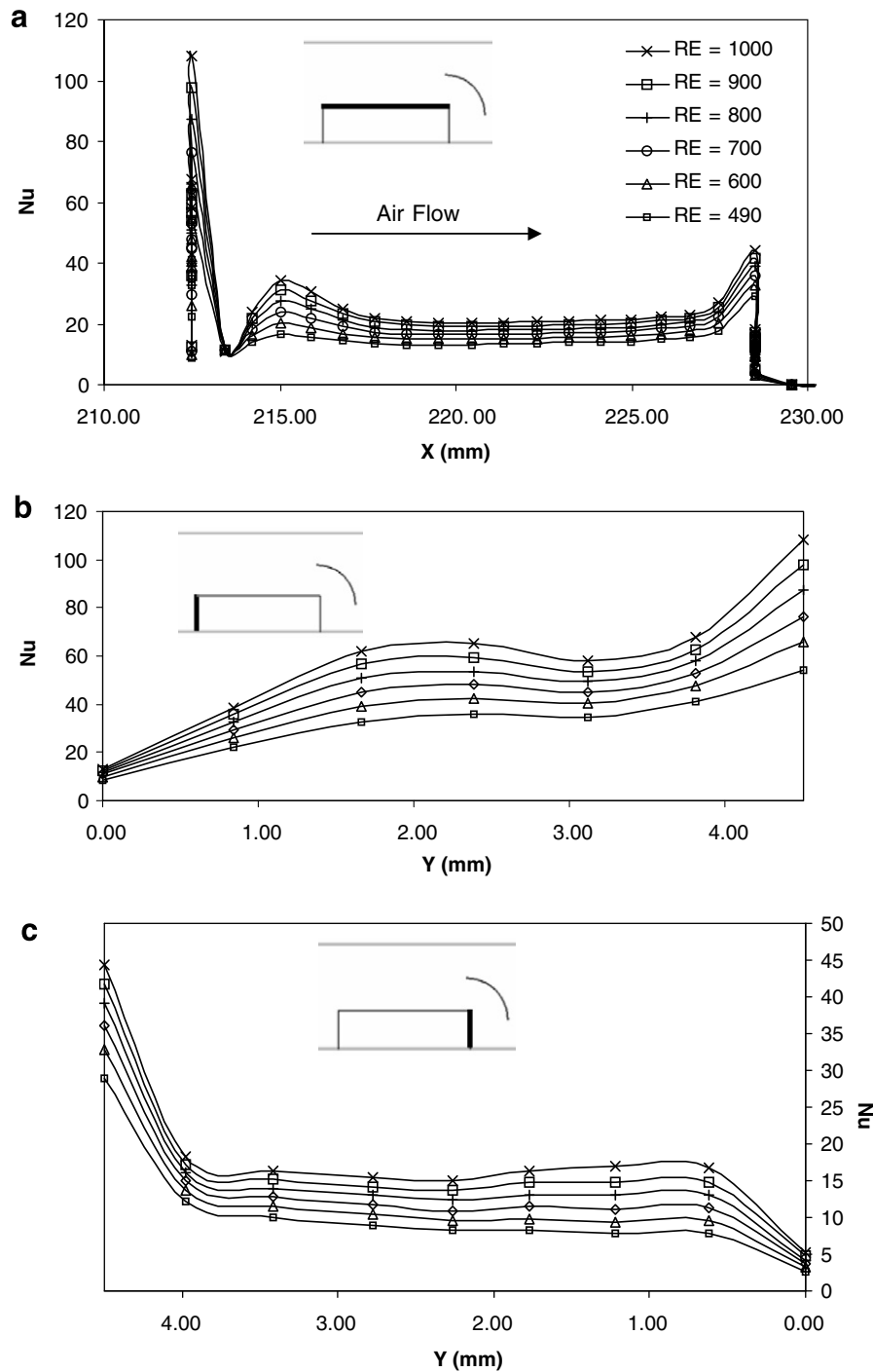


Fig. 12. Local Nusselt number for block 9 with deflector $R = L/5$ in the position $R_x = L/5$, $R_y = 4L/25$, for different Reynolds number (Re_D): (a) horizontal wall, (b) vertical front wall, (c) vertical back wall.

was expected, Fig. 12 shows that for a larger Reynolds number a larger local Nusselt number is obtained.

In Figs. 11b and 12b it is observed that the local Nusselt number increases towards the upper part of the vertical front wall, this is caused by the acceleration of the fluid that is leaving the deflector and for the instability that is generated when the fluid that is passing above the deflector and the fluid that is passing below the deflector mix. Figs. 11c and 12c show that the Nusselt number

diminishes toward the lower part of the vertical back wall, a value that is less than the local Nusselt numbers obtained at the vertical front wall and at the horizontal surface. This is due because some fluid gets trapped immediately after the block and deflector, generating recirculation.

Fig. 13 show that the global Nusselt number for the deflector $R = 5$ mm is almost identical to the global Nusselt number for the deflector $R = 4$ mm. These deflectors cause

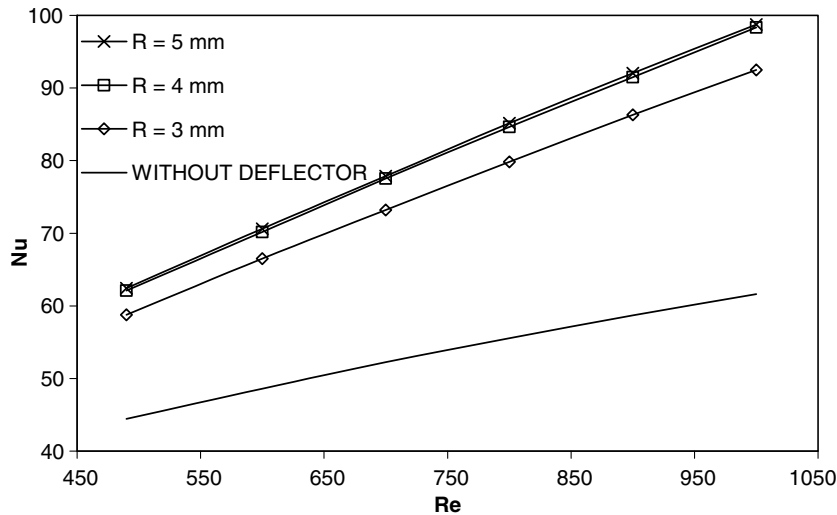


Fig. 13. Global Nusselt number vs. Reynolds number for different sizes of deflectors.

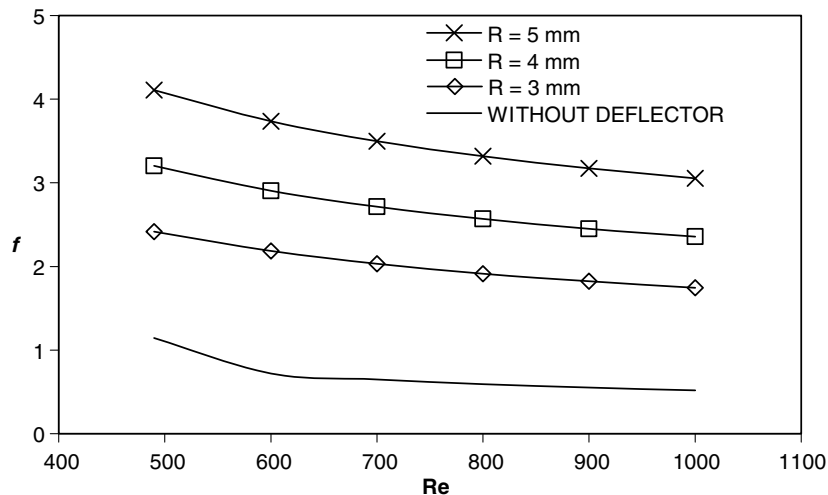


Fig. 14. Friction factor vs. Reynolds number.

approximately two times more increment in the global Nusselt number compared to when there are no deflectors. The deflector $R = 3$ mm causes approximately 1.5 times more increment in the global Nusselt number as compared to the case without deflector.

10. Friction coefficient

Fig. 14 shows the values obtained for the conditions analyzed with deflectors compared to those obtained without deflectors. It is observed that when the deflector is $R = 5$ mm, the friction factor is approximately four times larger than the channel of flat plates.

When $R = 4$ mm the friction factor is approximately 3 times larger than that for a channel without deflector, for the deflector $R = 3$ mm is approximately 2.5 times larger. The friction factor when $R = 5$ mm is approximately 1.5 times greater than when $R = 4$ mm.

In Fig. 13 it is shown that the global Nusselt number for the deflectors $R = 5$ mm and $R = 4$ mm, are almost identical. Since the channel with the deflector $R = 5$ mm cause larger friction than the deflector $R = 4$ mm, and the global Nusselt number for the deflector $R = 5$ mm is almost the same as that of the deflector $R = 4$ mm, it can be concluded that the use of the deflector $R = 4$ mm provides an optimum.

11. Conclusions

The geometry of the channel directly affects the thermal and hydraulic behavior of the fluid; the residence time of the particles within the secondary flow in the regions between the blocks can not be determined with certainty, nevertheless when the deflectors are used, the flow velocity increases in the areas between the blocks and therefore is diminished the fluid stagnation. Interestingly the recircula-

tion in the regions between the blocks has a smaller intensity when a deflector of smaller size is used (this is somehow logical, since when a smaller deflector is in position there will be a certain amount of deflected liquid that will try to follow the main flow path, therefore sending a smaller amount of liquid to the bottom zone between the blocks), nevertheless the use of larger deflectors causes a larger pressure gradient, generating unfortunately a larger friction loss. The deflectors generate better contours of temperature than those obtained in the channel without deflectors. It was found that to position the deflectors too close to the edge of the right corner of a block is not efficient, since the deflector would only be directing the flow to the area next to the vertical right wall of this block, not hitting the left side of the next block (which is the main purpose of the deflector, to hit areas where there could be flow stagnation). Stagnation could not be eliminated completely, however, when the deflectors are placed in an appropriate position, the heat transfer becomes more effective as compared to the case when there are not deflectors. Thus, horizontal channel of flat plates with blocks and deflectors in their interior, generates better heat transfer than the traditional channel. The results demonstrate that the flow through the channel of horizontal parallel flat plates with periodic insertion of heated blocks and deflectors forms a highly complex pattern; however, the time that the particles of the secondary fluid remain in the regions between the heated blocks can not be known for sure. The recirculation in the regions between the blocks is strongly influenced by the Reynolds number (Re_D), due to a change in the sign of the pressure gradient. Therefore, at low Reynolds numbers, greater stagnation of fluid will be presented at any position and for any size of the deflector. It is not recommended to use the deflectors in a position above $R_y = 7L/50$, $R_y = 9L/50$ and $R_y = L/5$ for the deflectors $R = 3L/25$, $R = 9L/50$ and $R = 11L/50$, respectively. This is because the flow deflected by these deflectors does not reach completely the bottom of the section between heated blocks. It is also not recommended to use deflectors in a position far from $R_x = 3L/10$, for the deflectors $R = 3L/25$, $R = 4L/25$ and $R = L/5$, since these deflectors would create flow stagnation, recirculating flow and therefore leading to deficient heat transfer. Analyzing Figs. 12–14, it is concluded that the profile which obtains the best heat transfer is for the deflector $R = L/5$. The use of these deflectors would, however, generate larger pressure gradients as compared to using smaller deflectors. On the other hand this deflector ($R = L/5$) would generate a high average Nusselt number. Interestingly, this Nusselt number is almost the same to

the one obtained using a deflector of $R = 4L/25$ (which produces less friction). Therefore it could be concluded that the best deflector is $R = 4L/25$.

References

- [1] C. Herman, E. Kang, Comparative evaluation of three heat transfer enhancement strategies in a grooved channel, *Heat Mass Transfer* 37 (2001) 563–575.
- [2] C. Herman, Experimental visualization of temperature fields and study of heat transfer enhancement in oscillatory flow in a grooved channel, *Heat Mass Transfer* 37 (2001) 87–99.
- [3] C. Herman, E. Kang, Heat transfer enhancement in a grooved channel with curved vanes, *Int. J. Heat Mass Transfer* 45 (18) (2002) 3741–3757.
- [4] C. Herman, E. Kang, An experimental study of convective heat transfer enhancement in a grooved channel using cylindrical eddy promoters, *J. Enhanc. Heat Transfer* 8 (2002) 1–19.
- [5] K. Billen, S. Yapici, Heat transfer from a surface fitted with rectangular blocks at different orientation angle, *Heat Mass Transfer* 38 (2002) 649–655.
- [6] C.H. Amon, B.B. Mikic, Numerical prediction of convective heat transfer in self-sustained oscillatory flows, *J. Thermophys. Heat Transfer* 4 (2) (1990) 239–246.
- [7] B. Farhanieh, C. Herman, B. Sunden, Numerical and experimental analysis of laminar fluid flow and forced convection heat transfer in a grooved duct, *Int. J. Heat Mass Transfer* 36 (6) (1993) 1609–1617.
- [8] J.S. Nigen, C.H. Amon, Forced convective cooling enhancement of electronic package configurations through self-sustained oscillatory flows, *ASME J. Electron. Pack.* 115 (1993) 356–365.
- [9] Kang-Hoon Ko, N.K. Anand, Use of porous baffles to enhance heat transfer in a rectangular channel, *Int. J. Heat Mass Transfer* 46 (22) (2003) 4191–4199.
- [10] T.M. Liou, S.H. Chen, Turbulent heat and fluid flow in a passage disturbed by detached perforated ribs of different heights, *Int. J. Heat Mass Transfer* 41 (12) (1998) 1795–1806.
- [11] M. Molki, A.R. Mostoufizadeh, Turbulent heat transfer in rectangular ducts with repeated-baffle blockages, *Int. J. Heat Mass Transfer* 32 (8) (1989) 1491–1499.
- [12] C.H. Amon, D. Majumdar, C.V. Herman, F. Mayinger, B.B. Mikic, D.P. Sekulic, Numerical and experimental studies of self-sustained oscillatory flows in communicating channels, *Int. J. Heat Mass Transfer* 35 (11) (1992) 3115–3129.
- [13] T. Adachi, H. Uehara, Linear stability analysis of flow in a periodically grooved channel, *Int. J. Numer. Methods Fluids* 41 (6) (2003) 601–613.
- [14] A.M. Anderson, R.J. Moffat, Direct air cooling of electronic components: reducing component temperatures by controlled thermal mixing, *J. Heat Transfer* 113 (1991) 56–62.
- [15] Wu-Shung Fu, Bao-Hong Tong, Numerical investigation of heat transfer characteristics of the heated blocks in the channel with a transversely oscillating cylinder, *Int. J. Heat Mass Transfer* 47 (2) (2004) 341–351.
- [16] D.B. Tuckerman, R.F.W. Pease, High-performance heat sinking for VLSI, *Electron Dev. Lett. IEEE* 2 (5) (1981) 126–129.
- [17] Takahiro Adachi, Shougo Hasegawa, Transition of the flow in a symmetric channel with periodically expanded grooves, *Int. J. Heat Mass Transfer* 61 (8) (2006) 2721–2729.